

(1) (A)

AD-A255 818



AD _____

**CHOLINERGIC NEUROTRANSMISSION IN THE
MAMMALIAN RETINA**

ANNUAL SUMMARY REPORT

Roberta G. Pourcho

January 30, 1988

**Supported by
U.S. ARMY MEDICAL RESEARCH AND DEVELOPMENT COMMAND
Fort Detrick, Frederick, Maryland 21701-5012**

DTIC
SEP 9 1988

Contract No. DAMD 17-83-C-3192

**Wayne State University
Detroit, Michigan 48202**

DOD DISTRIBUTION STATEMENT

Approved for public release: Distribution unlimited.

**The findings in this report are not to be construed as an
official Department of the Army position unless so
designated by other authorized documents.**

92 9 29 055

371550

92-26166



3381

REPORT DOCUMENTATION PAGE

Form Approved
OMB No. 0704-0188

a. REPORT SECURITY CLASSIFICATION Unclassified		1b. RESTRICTIVE MARKINGS	
a. SECURITY CLASSIFICATION AUTHORITY		3. DISTRIBUTION/AVAILABILITY OF REPORT Approved for public release; distribution unlimited.	
b. DECLASSIFICATION/DOWNGRADING SCHEDULE		5. MONITORING ORGANIZATION REPORT NUMBER(S)	
4. PERFORMING ORGANIZATION REPORT NUMBER(S)		7a. NAME OF MONITORING ORGANIZATION	
1a. NAME OF PERFORMING ORGANIZATION Wayne State University	6b. OFFICE SYMBOL (if applicable)	7b. ADDRESS (City, State, and ZIP Code)	
1c. ADDRESS (City, State, and ZIP Code) Detroit, Michigan 48202		9. PROCUREMENT INSTRUMENT IDENTIFICATION NUMBER Contract No. DAMD17-83-C-3192	
1a. NAME OF FUNDING/SPONSORING ORGANIZATION U.S. Army Medical Research & Development Command	8b. OFFICE SYMBOL (if applicable)	10. SOURCE OF FUNDING NUMBERS	
1c. ADDRESS (City, State, and ZIP Code) Fort Detrick Frederick, Maryland 21702-5012		PROGRAM ELEMENT NO. 61102A	PROJECT NO. 3M1- 61102BS11
		TASK NO. AA	WORK UNIT ACCESSION NO. 008
11. TITLE (Include Security Classification) Cholinergic Neurotransmission in the Mammalian Retina			
12. PERSONAL AUTHOR(S) Roberta G. Pourcho			
13a. TYPE OF REPORT Annual Report	13b. TIME COVERED FROM 9/30/85 TO 12/31/87	14. DATE OF REPORT (Year, Month, Day) 1988 January 30	15. PAGE COUNT 35
16. SUPPLEMENTARY NOTATION			
17. COSATI CODES		18. SUBJECT TERMS (Continue on reverse if necessary and identify by block number)	
FIELD	GROUP	SUB-GROUP	
06	15		
06	01		
		RAV; Lab animals; morphology; retina; neurotransmitters; acetylcholine; organophosphates: chemical defense	
19. ABSTRACT (Continue on reverse if necessary and identify by block number)			
<p>The cholinergic cells in the retina consist of matching subpopulations of amacrine and displaced amacrine cells which ramify narrowly in the inner plexiform layer (IPL). Previous cytochemical studies revealed that the hydrolytic enzyme acetylcholinesterase (AChE), which terminates the action of acetylcholine (ACh), is more widespread in its distribution than the enzyme choline acetyltransferase (ChAT), which is responsible for ACh synthesis. Cytochemical techniques were utilized to further define the sites of cholinergic interaction in the retina. Autoradiographic studies showed that both the muscarinic receptor ligand (3H)propylbenzyl choline mustard and the putative nicotinic receptor ligand (3H)alpha-bungarotoxin bind preferentially in the IPL.</p>			
20. DISTRIBUTION/AVAILABILITY OF ABSTRACT <input type="checkbox"/> UNCLASSIFIED/UNLIMITED <input type="checkbox"/> SAME AS RPT. <input type="checkbox"/> DTIC USERS		21. ABSTRACT SECURITY CLASSIFICATION Unclassified	
22a. NAME OF RESPONSIBLE INDIVIDUAL Virginia M. Miller		22b. TELEPHONE (Include Area Code) 301-619-7325	22c. OFFICE SYMBOL SGRD-RMI-S

Autoradiographic localization of (3H)soman showed the greatest label density in the IPL, with a laminar distribution similar to the zones of intense AChE activity. Retinas of cats exposed to soman by intravitreal injection showed a progressive destruction of neurons, with cells in the ganglion cell layer being most severely affected. These are the same neurons were also found to contain high levels of AChE activity.

Evidence for interaction of ACh with glycinergic neurotransmission was obtained from experiments in which (3H)glycine release from preloaded retinas was monitored by scintillation counting. Application of ACh caused an increased release of label. This release was blocked by curare, so appears to be mediated by nicotinic receptors. An interaction of AChE with the neuropeptide substance P was demonstrated from assays of retinas that had been exposed to the anticholinesterase compound diisopropylfluorophosphate (DFP). DFP-treated retinas consistently showed elevated levels of SP that may be attributed to a decreased level of hydrolysis of the neuropeptide in the absence of AChE. Interactions of AChE with neuropeptides such as SP may contribute to the long-term effects of exposure to anticholinesterase compounds.

SUMMARY

The cholinergic cells in the retina have been identified as matching subpopulations of amacrine and displaced amacrine cells which ramify narrowly in the inner plexiform layer (IPL). Previous cytochemical studies revealed that the hydrolytic enzyme acetylcholinesterase (AChE), which terminates the action of acetylcholine (ACh) is more widespread in its distribution than the enzyme choline acetyltransferase (ChAT), which is responsible for ACh synthesis. During the present reporting period, cytochemical techniques were utilized to further define the sites of cholinergic interaction in the retina.

Autoradiographic studies showed that binding of the muscarinic receptor ligand (3H)propylbenzilyl choline mustard was confined primarily to the IPL.

(3H)Alpha-bungarotoxin, a putative nicotinic receptor ligand, was also found to bind preferentially in the IPL. Laminar distributions of both ligands within the IPL were consistent with the ramification of cholinergic neurons.

Sites of action in the retina of the anticholinesterase organophosphorus compound soman were investigated by the use of autoradiography and by evaluation of the neurotoxic effects of this agent on neuronal morphology.

Autoradiographic localization of (3H)soman showed the greatest label density in the IPL, with a laminar distribution similar to the zones of intense AChE activity. Retinas of cats exposed to soman by intravitreal injection showed a progressive destruction of neurons, with cells in the ganglion cell layer being most severely affected. These are the same neurons which, although not cholinergic, were found to contain high levels of AChE activity.

Exposure of retinas to substances which affect levels of either ACh or AChE can be expected to influence a variety of neurotransmitter systems. Evidence for interaction of ACh with glycinergic neurotransmission was obtained from experiments in which (3H)glycine release from preloaded retinas was monitored by scintillation counting.

Application of ACh caused an increased release of label. This release was blocked by atropine, so appears to be mediated by muscarinic receptors. An increasing volume of evidence suggests that AChE participates not only in the inactivation of ACh but also in a variety of non-cholinergic functions. In order to investigate this possibility, levels of the neuropeptide substance P (SP) were determined by assay of retinas that had been exposed to the anticholinesterase compound diisopropylfluorophosphate (DFP). DFP-treated retinas consistently showed elevated levels of SP, with values ranging from 35-200% greater than those in control eyes. The increase in SP may be attributed to a decreased level of hydrolysis of the neuropeptide in the absence of AChE. Interactions of AChE with neuropeptides such as SP may contribute to the long-term effects of exposure to anticholinesterase compounds.

11

FOREWORD

In conducting the research described in this report, the investigator adhered to the "Guide for the Care and Use of Laboratory Animals," prepared by the Committee on Care and Use of Laboratory Animals of the Institute of Laboratory Animal Resources, National Research Council (DHEW Publication No. (NIH) 78-23, Revised 1978).

Citations of commercial organizations or trade names in this report do not constitute an official Department of the Army endorsement or approval of the products or services of these organizations.

DTIC QUALITY INSPECTED 3

A-1

TABLE OF CONTENTS

Summary	3
Foreword	5
Statement of problem	9
Background	9
Approach	10
Cytochemical studies	10
Biochemical studies	20
Conclusions	29
Recommendations	29
Literature cited	31
Glossary	33
Distribution list	35
Figures	
1. Distribution of (3H)PrBCM binding in the retina	12
2. Laminar distribution of (3H)PrBCM in the IPL	12
3. Distribution of (3H)alpha-bungarotoxin binding in the retina	13
4. Laminar distribution of (3H)alpha-bungarotoxin in the IPL	14
5. Distribution of (3H)soman binding in the retina	15
6. Laminar distribution (3H)soman in the IPL	15
7. Retina 4 hours after intravitreal injection of 0.1 ng soman	17
8. Retina 4 hours after intravitreal injection of 1.0 ng soman	18
9. Retina 4 hours after intravitreal injection of 10 ng soman	19
10. Retina 24 hours after intravitreal injection of 0.1 ng soman	20
11. Retina 24 hours after intravitreal injection of 1.0 ng soman	21
12. ACh-stimulated release of (3H)glycine	22
13. ACh-stimulated release of (3H)glycine blocked by curare	23
14. Calcium dependence of (3H)glycine release	23
15. Comparison of laminar distributions of ChAT, AChE and SP in cat IPL	24
Table 1. Levels of SP-IR material in DFP-treated and untreated rabbit retinas	26

STATEMENT OF PROBLEM:

Acetylcholine (ACh)* is a major neurotransmitter in the retina and throughout the rest of the central nervous system (CNS). The ACh-hydrolyzing enzyme acetylcholinesterase (AChE) plays an important role in terminating the effects of ACh. In addition, AChE is known to be present in locations which receive no cholinergic input. Both the cholinergic and non-cholinergic effects of AChE are at risk upon exposure to organophosphate compounds, including substances which may be considered for military use.

Our studies in the cat retina have identified a subpopulation of amacrine and displaced amacrine cells which are cholinergic (1,2). These cells exhibit the distinctive starburst-like morphology which characterizes cholinergic cells in other retinas, and they ramify in two narrow bands within the inner plexiform layer (IPL). Cytochemical studies have demonstrated that these cells are able to synthesize (3H)ACh from (3H)choline and that they contain both AChE and the ACh-synthesizing enzyme, choline acetyltransferase (ChAT). However, the cholinergic neurons ramify at 20% and 50% depth levels within the IPL whereas the major bands of AChE activity are located at 0-6% and 64-78% depth levels (3,4). In view of these findings, it is important to determine the distribution of receptor sites for ACh as well as the distribution of binding sites for the anticholinesterase compound soman.

The neurotoxic effects of soman were also studied. Release studies were carried out in order to provide additional information about the post-synaptic relationships of cholinergic cells. Finally, the relationships of AChE and anti-AChE substances with levels of retinal neuropeptides were investigated.

BACKGROUND:

The vertebrate retina has often been employed as a model system for the study of neurotransmitters and their interactions. The ready accessibility and laminar organization of the retina make it particularly valuable for these studies. Ongoing work in this and other laboratories has led to the localization of many neurotransmitters in specific neuronal subpopulations. Among the substances identified as transmitters in the retina are ACh, dopamine, glycine, gamma-aminobutyric acid, and substance P (SP).

Recently, it has become evident that many neurons contain multiple neurotransmitters or neuromodulators and that the function of each cell is related to its total neurochemical content. While colocalization studies have proceeded rapidly in retinas of many non-mammalian vertebrates, it is only within the past months that we have been able to provide confirmation of the phenomenon in a mammalian (cat) retina (5). How multiple transmitters

*Abbreviations are defined in the glossary on p. 33.

cooperate in neuronal function is a major problem for future research.

In line with the evidence for individual cells possessing multiple transmitters are data indicating that AChE, typically thought of in terms of cholinergic function, may also participate in the processing of neuropeptides. This processing may include both the generation of functional peptides from precursor molecules and the hydrolytic inactivation of the peptides. In support of such a possibility, it has recently been shown that AChE may undergo autolysis to generate a trypsin-like activity (6).

Retinal studies exploring possible interactions between AChE and neuropeptides have focused particularly on SP. It has been suggested that, like enkephalin, SP may be generated from a precursor molecule through the hydrolytic action of AChE (7). Alternatively, AChE may serve to inactivate SP by hydrolysis of the peptide itself (8). In either case, anti-AChE organophosphates would be expected to influence not only cholinergic function but also peptidergic function within the retina. Thus, an exposure to anticholinesterase compounds may lead to an imbalance in multiple neurotransmitter systems.

APPROACH:

As in previous years (1,3), these studies have employed two lines of investigation. Cytochemical techniques were used to localize muscarinic and nicotinic ACh receptors in the retina and to determine the sites of binding of (3H)soman. In addition, the effects of intravitreal injection of soman on retinal morphology were investigated. In order to confirm previous indications that ACh influences the release of glycine, retinas that had been preloaded with (3H)glycine were treated with ACh and the radioactivity in the supernatant was monitored by scintillation counting. Interactions between AChE and SP were explored by treating retinas with the anticholinesterase compound diisopropylfluorophosphate (DFP) and assaying changes in the concentrations of both AChE and SP.

Cytochemical Studies:

1. Autoradiographic localization of muscarinic receptors using (3H)propylbenzilylcholine mustard [(3H)PrBCM].

In order to more fully characterize cholinergic pathways within the retina, (3H)PrBCM was used to localize muscarinic receptors. This compound is widely used as a specific ligand for muscarinic sites. Light microscopic autoradiographic techniques were used to visualize the location of (3H)PrBCM binding within the retina. The autoradiographs were analyzed by the use of computer-assisted procedures to define the laminar distribution of receptors within the IPL.

Materials and Methods. The cats used in this study were random adult cats. Siamese cats were excluded because of documented visual abnormalities. Freshly dissected cat retinas were preincubated for 30 minutes at room temperature in bicarbonate buffer (9) with continuous gassing with 95% oxygen, 5% carbon dioxide. Razor-blade slices of retina were then incubated for 30 minutes in 2 ml of the same buffer containing 25 nM (3H)PrBCM. The PrBCM had been previously activated at a concentration of 1 uM in 10 mM phosphate buffer, pH 7.4, for 1 hour at room temperature and kept on ice until used. Control retinas were treated similarly but were incubated for 5 minutes in 1 uM atropine prior to addition of (3H)PrBCM. To stop the reaction, 5 ml ice-cold buffer was added to each sample. The tissue was washed, then fixed in 2% paraformaldehyde and 2% glutaraldehyde in 0.1 M phosphate buffer for 1-2 hours, postfixed in 1% osmium tetroxide, dehydrated rapidly through graded alcohols and embedded in Epon-Araldite. One-micron sections were collected on glass slides and dipped into a 1:3 dilution of molten Ilford K-5 emulsion. Autoradiographs were developed after 10-25 weeks.

Grain densities were determined for defined retinal layers and the values normalized in relation to the mean grain densities across the retina. Corrected values were calculated by subtracting normalized relative grain densities of control samples from values obtained for the experimental samples. To determine the distribution of label within the IPL, locations of silver grains were plotted on a HIPAD digitizing pad (Houston Instruments, Austin, TX) interfaced with a Cromemco 6800 microcomputer (Cromemco, Inc., Mountain View, CA). Reference lines were established at the outer and inner borders of the IPL, and individual grains were assigned to bins representing 1/20 of the total thickness of the IPL.

Results. Retinas incubated with (3H)PrBCM alone showed labeling in all retinal layers, with a preferential accumulation in the IPL. Controls incubated in the presence of atropine showed a more uniform labeling across the retina. Relative grain densities for the various retinal layers from a typical experiment are shown in Fig. 1. The plot showing corrected values emphasizes binding within the IPL. When the distribution of (3H)PrBCM was plotted across the IPL, it was apparent that the greatest concentrations were at the 15-55% depth levels (Fig. 2).

Discussion. The level of specific binding of (3H)PrBCM in the IPL was twice that seen in other retinal layers. Computer assisted analysis indicated a further limitation to middle and outer strata. The 15-55% depth band coincides with the location of cholinergic fibers which have been shown by choline acetyltransferase (ChAT) staining to ramify in two narrow strata at 20% and 50% levels. These findings support the conclusion of other investigators (10) that muscarinic cholinergic function in the mammalian retina is centered within the IPL.

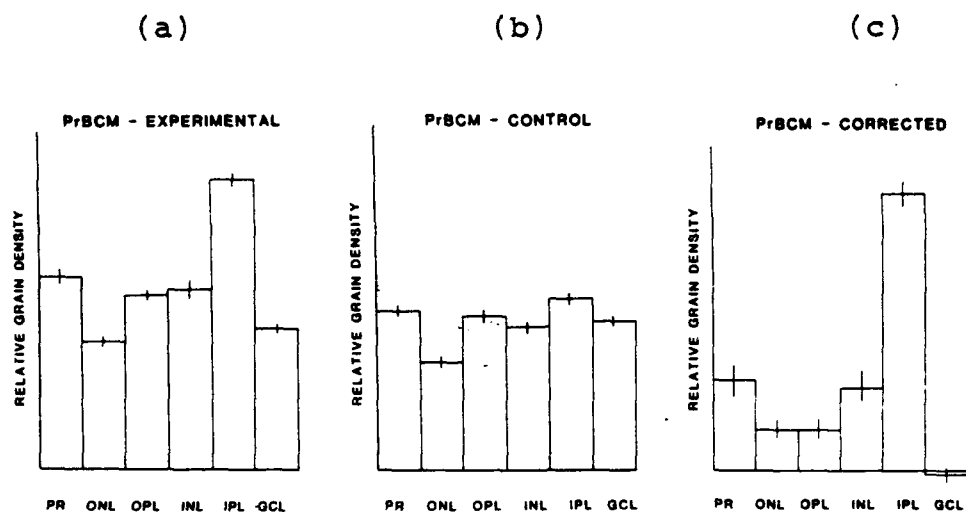


Fig. 1. Distribution of $(3H)PrBCM$ binding in the retina. Histograms show relative grain densities for retinas incubated with $(3H)PrBCM$ alone (a) and for retinas incubated with $(3H)PrBCM$ in the presence of atropine. Corrected values are plotted in (c). Each experiment was repeated a minimum of three times with counts being made from eight representative sections. PR, photoreceptor layer; ONL, outer nuclear layer; OPL, outer plexiform layer; INL, inner nuclear layer; IPL, inner plexiform layer; GCL, ganglion cell layer.

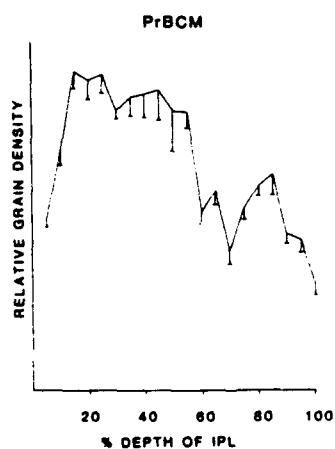


Fig. 2. Laminar distribution of $(3H)PrBCM$ in the IPL. Labeling was concentrated between 15 and 55% depth levels.

2. Autoradiographic localization of putative nicotinic ACh receptors using (3H)alpha bungarotoxin.

The distribution of presumptive nicotinic receptors in the retina was studied through the use of (3H)alpha-bungarotoxin. Light microscopic autoradiographs were analyzed by computer-assisted techniques to determine the distribution of labeling within the IPL.

Materials and Methods. Freshly dissected cat retinas were incubated in bicarbonate buffer containing 10^{-8} M (3H)alpha-bungarotoxin and processed as described above. Controls were preincubated in 10^{-5} M nicotine to which (3H)alpha-bungarotoxin was added after 5 minutes. After washing in buffer, samples were prepared for autoradiography and analyzed as described above.

Results. Labeling in retinas incubated with (3H)alpha-bungarotoxin alone was concentrated in the IPL (Fig. 3) whereas its distribution in retinas pretreated with nicotine was more diffuse through all layers. As with PrBCM, the corrected plot emphasizes the labeling of the IPL. Computer-assisted analysis of the variations within the IPL (Fig. 4) showed the greatest concentration near the 55% depth level, with a broader band from 20-55%.

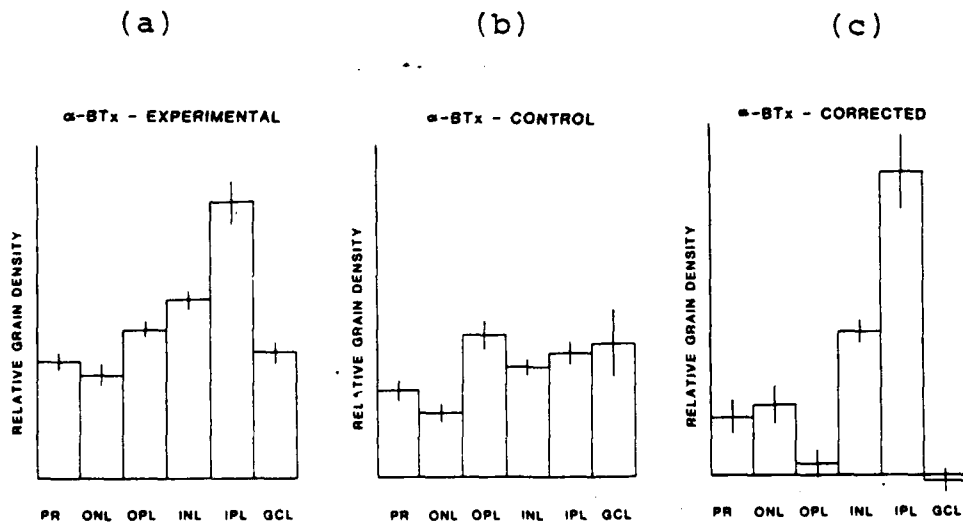


Fig. 3. Distribution of (3H)alpha-bungarotoxin binding in the retina. Histograms show relative grain densities for retinas incubated with (3H)alpha-bungarotoxin alone (a) and for retinas incubated with (3H)alpha-bungarotoxin in the presence of nicotine. Corrected values are plotted in (c). Sample size and abbreviations are as indicated for Fig. 1.

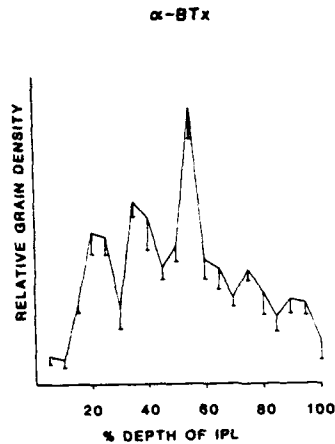


Fig. 4. Laminar distribution of (3H)alpha-bungarotoxin in the IPL. Labeling was most concentrated at a 55% depth level.

Discussion. Like the PrBCM labeling, alpha-bungarotoxin binding was concentrated in the IPL, with very little binding in other retinal layers. The greatest concentration of label was seen at the 55% depth level. This suggests a correspondence with the ramification of cholinergic displaced amacrine cells which form a narrow band near the 50% depth level (2). Although alpha-bungarotoxin has been used extensively for the study of cholinergic systems, it is recognized that this toxin does not block neurotransmission in the central nervous system. This observation casts some doubt on the significance of bungarotoxin labeling, and results must be interpreted with caution.

3. Autoradiographic localization of (3H)soman.

The autoradiographic localization of soman was carried out and analyzed using similar techniques to those employed for localization of muscarinic and putative nicotinic receptors. Comparisons were made with the distribution of both cholinergic neurons and AChE activity.

Materials and methods. Freshly dissected cat retinas were incubated for 20-60 minutes in 5 ml oxygenated bicarbonate buffer containing soman at concentrations ranging from 10^{-5} to 10^{-6} M. At the end of the incubation, samples were rinsed in 0.1 M phosphate buffer, fixed in 3% glutaraldehyde and 2% paraformaldehyde, postfixed with 1% osmium tetroxide, and processed for autoradiography as described above. Exposure times ranged from 16-29 weeks, after which autoradiographs were developed and grain density analyzed.

Results. Preliminary analysis of the autoradiographs showed that grain densities were essentially the same in all retinal layers of samples incubated with 10^{-5} or

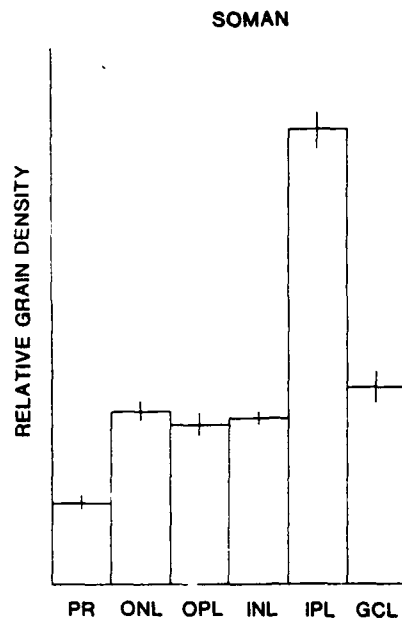


Fig. 5. Distribution of (3H)soman binding in the retina as determined from incubation of tissue in 10^{-7} M (3H)soman. The greatest label density was seen in the IPL. Abbreviations are defined in Fig. 1.

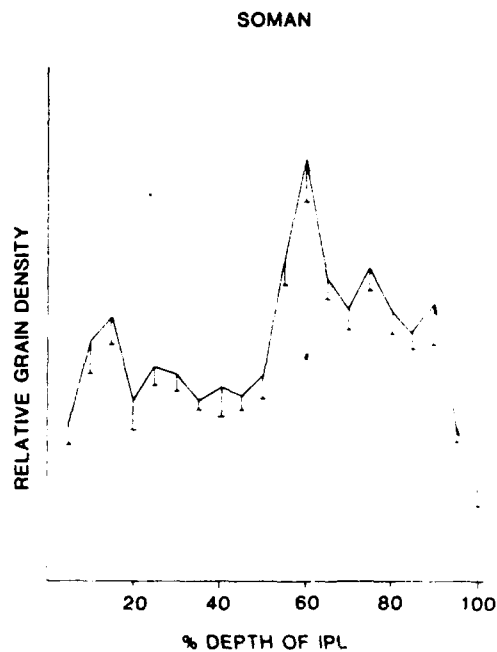


Fig. 6. Laminar distribution of (3H)soman in the IPL. A narrow band of labeling was seen at the 15-20% depth level, with a wider band from 55-90%. A sharp peak appeared at 60%.

10^{-6} M soman. However, the grain density in samples incubated in 10^{-7} M soman showed marked differences among the retinal layers. Labeling in the IPL was twice as heavy as in any of the other layers and nearly 5 times as great as the labeling of photoreceptor inner and outer segments. These values are plotted in Fig. 5. These data are summarized from a total of 37,511 silver grains over 16 representative sections of retina. Further subdivision of the IPL into 20 bins showed that the greatest concentration was at the 60% depth level, with lesser peaks at 10-15% and 55-90% (Fig. 6).

Discussion. Soman was found to bind preferentially within the IPL of the cat retina, with relatively little binding in other retinal layers. Within the IPL, labeling was concentrated in two bands, a wide band extending from the 55-90% depth levels and a smaller band at 10-15%. These localizations are more similar to previously reported localizations of AChE activity than to the narrow bands of ChAT activity (3,4). Thus, the autoradiographic localization of soman is consistent with its interaction with sites of AChE activity in retinal tissue, even when those sites extend beyond the regions of direct cholinergic input.

4. Neurotoxicity of soman.

Studies of soman neurotoxicity were conducted in vivo and retinas were analyzed to compare the distribution of soman's degenerative effects with the known distributions of cholinergic neurons and AChE activity.

Materials and Methods. Adult cats were anesthetized with Ketamine and sodium pentobarbital and given intravitreal injections of soman in amounts ranging from 0.1-10 ng. Some animals were maintained for only 4 hours after injections and these were kept under anesthesia for the duration of the experiment. Others, which received smaller doses (0.1-1.0 ng), were allowed to regain consciousness and, since they exhibited no apparent discomfort, were kept for 24 hours before being sacrificed by overdose of sodium pentobarbital and the eyes removed. Retinas were fixed in 3% glutaraldehyde and 2% paraformaldehyde in 0.1 M phosphate buffer, postfixed in 1% osmium tetroxide, and embedded in Epon-Araldite. One-micron sections were cut for light microscopy and stained with Richardson's stain.

Results. Animals that received a 10-ng intravitreal injection of soman showed excessive production of mucus from the respiratory tract and pronounced lacrimal secretion. These animals were maintained under anesthesia to avoid discomfort. In contrast, little if any evidence of systemic involvement was observed in cats that received smaller doses of soman (0.1-1.0 ng). These animals appeared normal and were allowed to regain consciousness.

Microscopic examination of retinas from animals exposed

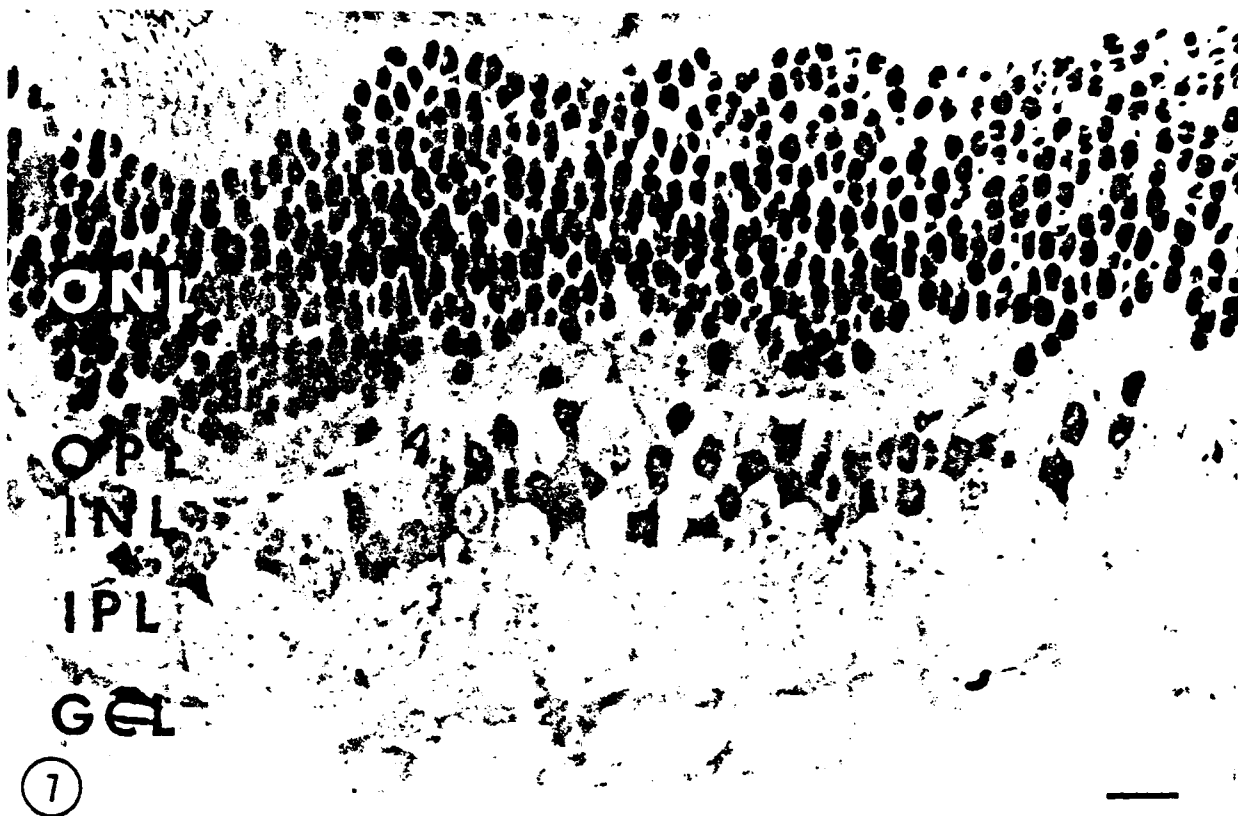


Fig. 7. Retina 4 hours after intravitreal injection of 0.1 ng soman. A small amount of vacuolation is evident in the ganglion cell layer (GCL). ONL, outer nuclear layer; OPL, outer plexiform layer; INL, inner nuclear layer; IPL, inner plexiform layer. Bar 10 um.

for 4 hours to soman in increasing concentrations showed a gradual increase in the amount of destruction of neuronal elements. Animals that received intravitreal injections of 0.1 ng soman showed some vacuolation in the GCL but very little indication of damage in other retinal layers (Fig. 7). Retinas treated with 1.0 ng soman for the same time period showed an increased amount of vacuolation in the GCL (Fig. 8). Retinas exposed to 10 ng soman showed more widespread destruction, with vacuolation extending into the OPL (Fig. 9). Ganglion cells appeared to be severely damaged with condensed cytoplasm and pyknotic nuclei.

The amount of destruction resulting from the smaller amounts of soman became more apparent in retinas processed 24 hours following the injections. Retinas from animals that received 0.1 ng soman and were maintained for a 24-hour period showed much extensive vacuolation in the GCL, with apparent loss of many ganglion cells (Fig. 10). Large spaces were also seen in the INL and IPL. Exposure of retinas to a single injection of 1.0 ng soman for a 24-hour

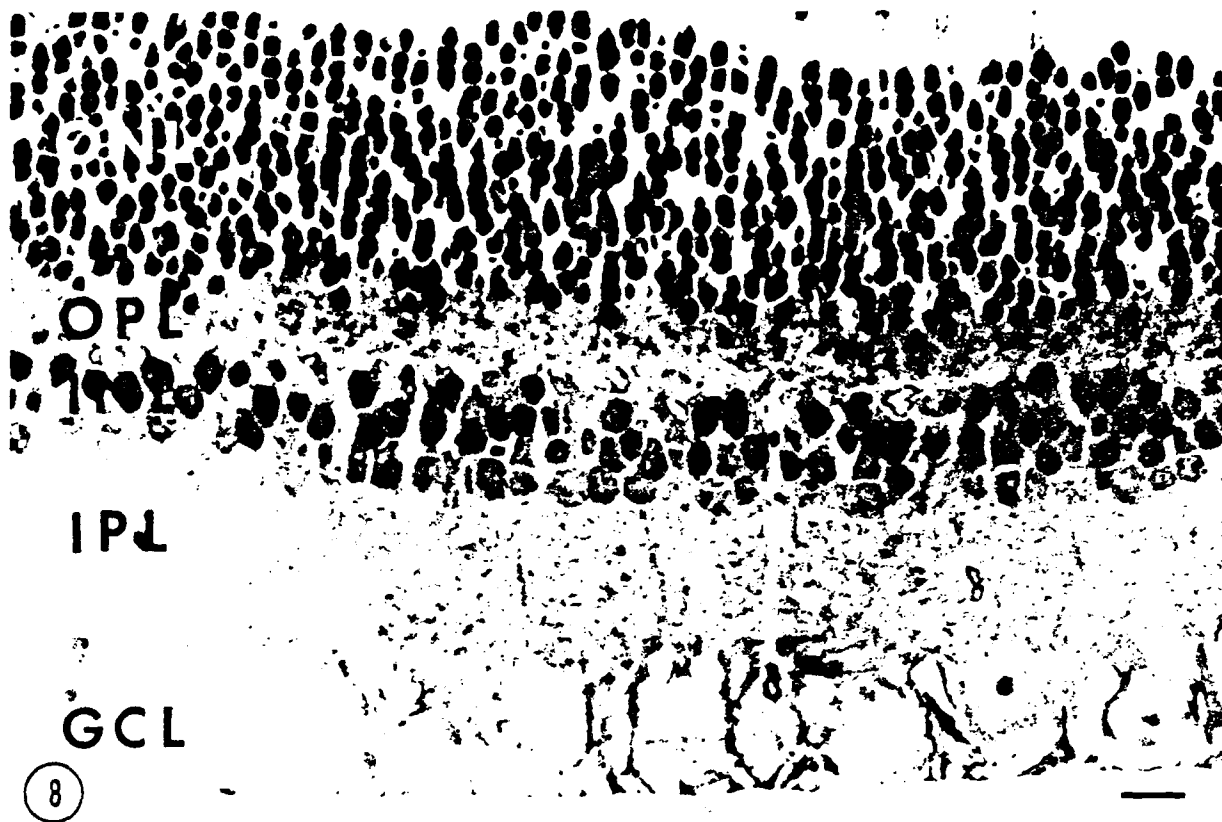


Fig. 8. Retina 4 hours after intravitreal injection of 1.0 ng soman. An increased amount of vacuolation is seen in the GCL (ganglion cell layer), with little visible damage in other retinal layers. ONL, outer nuclear layer, OPL, outer plexiform layer; INL, inner nuclear layer; IPL, inner plexiform layer. Bar 10 μ m.

period resulted in wide spread destruction involving massive breakdown of cells and fibers with hemorrhage into the tissue (Fig. 11). Vacuolation extended through the IPL and into the INL. Muller cells, the radial glia of the retina, were somewhat more resistant than many of the neurons although their processes often appeared darker than normal.

Discussion. The neurotoxic effects of soman were much more apparent in retinas after 24 hours of exposure than after 4 hours. Some of these increases may have been due to delayed diffusion of the agent into the tissue. However, it is more likely that the deleterious effects were initiated within the first 4-hour interval but did not become obvious until a later time.

The most striking change in retinas exposed to soman was the vacuolation in the GCL and the destruction of most of the ganglion cells. Some amacrine cells were also lost. The cells that appear most affected by soman poisoning are the same neurons which previously have been shown to contain AChE, the enzyme known to be inactivated by soman. Thus, the AChE-containing cells appear to be most sensitive to

anticholinesterase organophosphate poisoning. As noted previously, these cells include both cholinergic amacrine and displaced amacrine cells as well as the entire population of neurons in the GCL. The extensive destruction caused by soman suggests that this agent works against AChE, not only in those cells which participate in cholinergic neurotransmission, but also in those cells in which AChE has other, presumably non-cholinergic, functions.

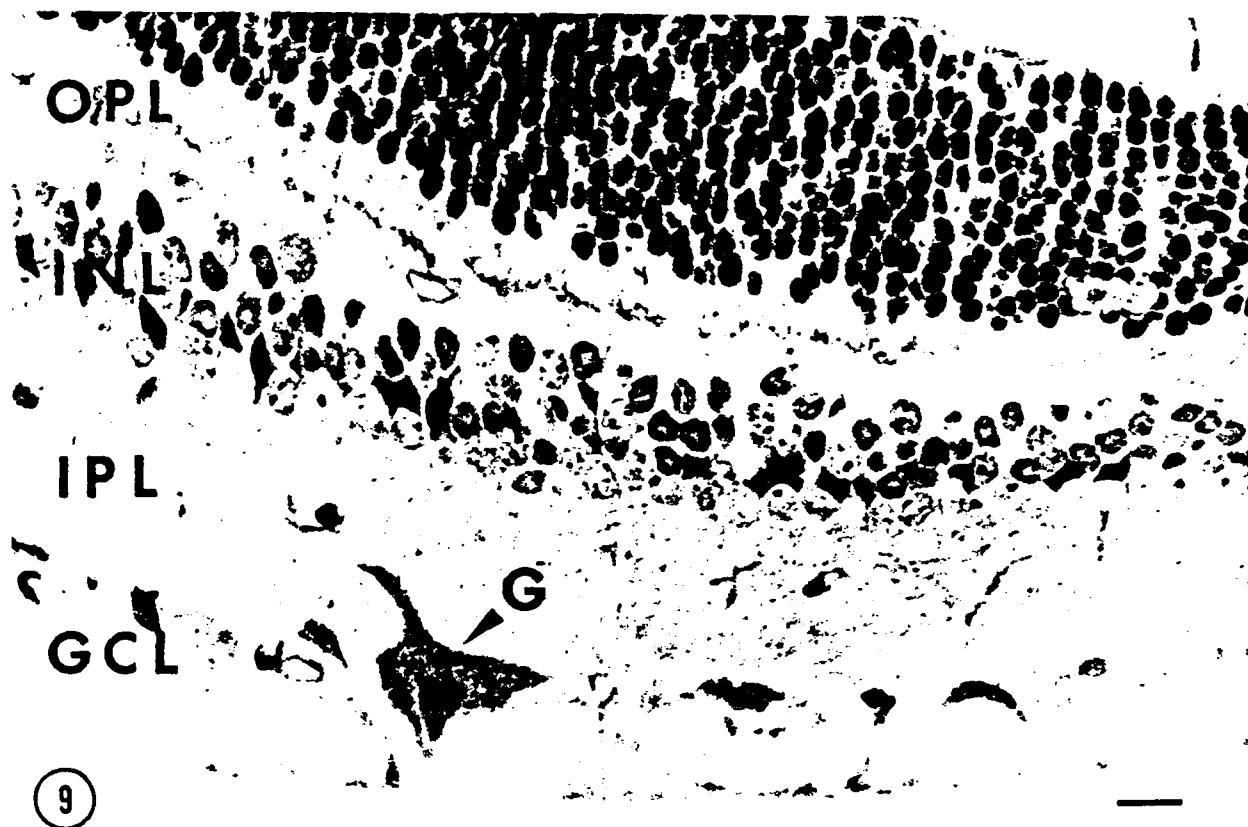


Fig. 9. Retina 4 hours after intravitreal injection of 10 ng soman. Retinal destruction is more widespread than with lower doses and includes not only the GCL (ganglion cell layer) but also the outer retina as far as the OPL (outer plexiform layer). INL, inner nuclear layer; IPL, inner plexiform layer. Bar 10 um.

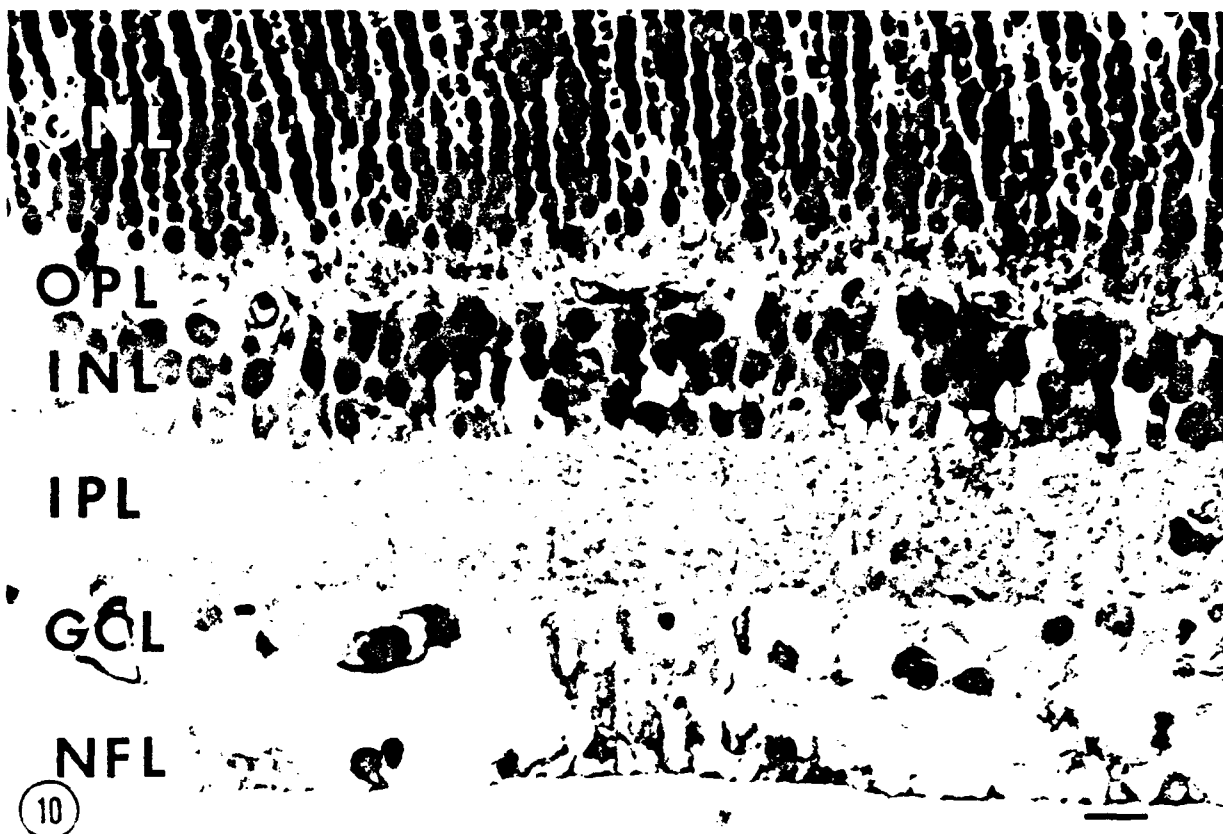


Fig. 10. Retina 24 hours after intravitreal injection of 0.1 ng soman. Extensive vacuolation is seen in the GCL (ganglion cell layer) and many cells appear to have been destroyed, although bundles of ganglion cell axons in the NFL (nerve fiber layer) appear intact. Evidence of cell loss can also be seen in the INL (inner nuclear layer). ONL, outer nuclear layer; OPL, outer plexiform layer; IPL, inner plexiform layer. Bar 10 μ m.

Biochemical Studies

1. Effects of ACh application on glycine release in the retina.

In order to determine whether changes in ACh levels, including those initiated by anticholinesterase compounds, would induce changes in other neurotransmitter systems, the effects of ACh on glycine release were studied in isolated retinas.

Materials and Methods. Cats were anesthetized with Ketamine and sodium pentobarbital and given intravitreal injections of 100 μ Ci (3 H)glycine. After a period of 3-4 hours during which the radiolabeled material was allowed to diffuse into the retina, the animals were sacrificed by overdose of sodium pentobarbital and the retinas removed.

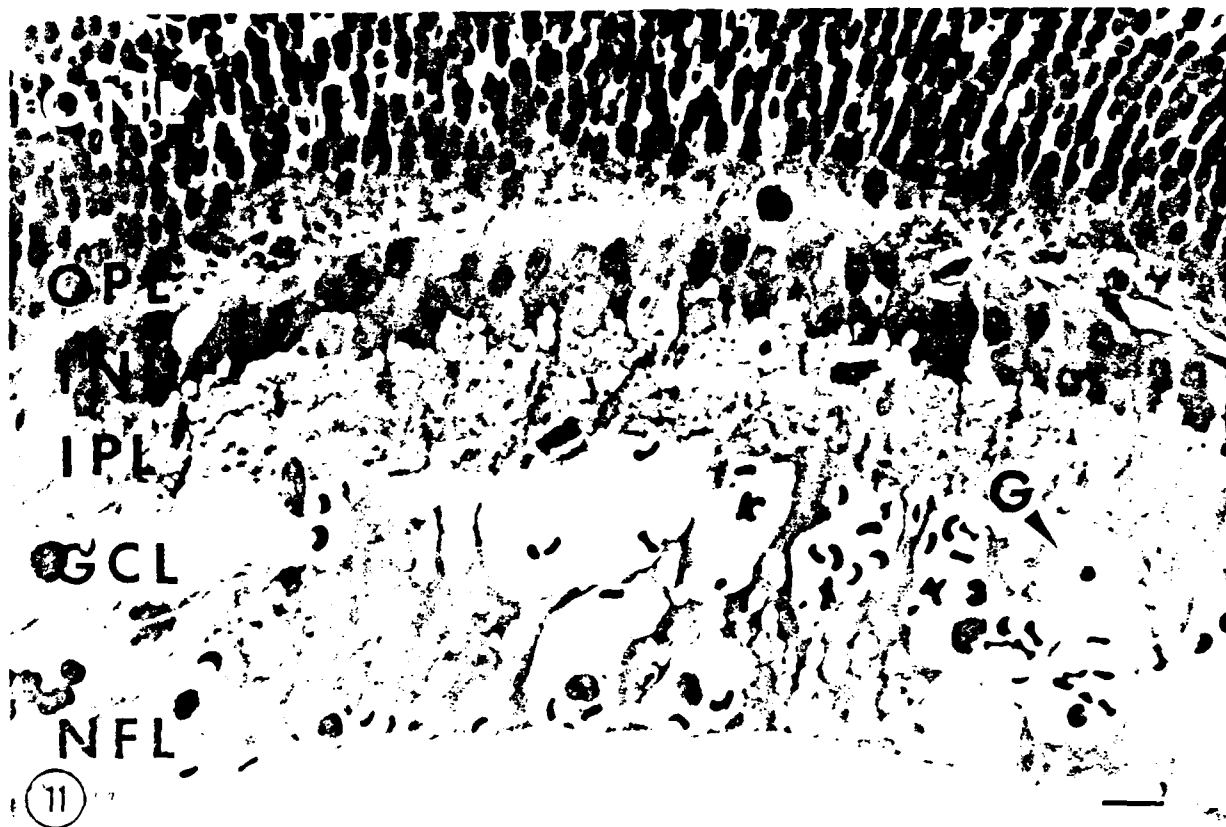


Fig. 11. Retina 24 hours after intravitreal injection of 1.0 ng soman. Massive destruction of the retina is evident, with bleeding into the tissue. In the GCL (ganglion cell layer), only an occasional cell body (G) can be seen. Vacuolation extends through the IPL (inner plexiform layer) and into the INL (inner nuclear layer). ONL, outer nuclear layer; OPL, outer plexiform layer; NFL, nerve fiber layer. Bar 10 μ m.

Each retina was cut in half and immersed in oxygenated bicarbonate buffer (9) for 20 minutes to allow free glycine to be washed out of the tissue. Subsequently the tissue was manipulated through 10 successive washes at 5-minute intervals. Each wash utilized a total volume of 2 ml and all samples were assayed for radioactivity by scintillation counting. Vial #5 in each series typically contained 1 mM ACh whereas vial #6 returned the tissue to fresh buffer. In order to determine if the ACh effect was mediated by nicotinic or muscarinic receptors, the protocol was repeated using buffer containing 10 mM curare and in buffer containing 10 mM atropine. The effects of each of these blockers on the glycine release curve was plotted. In order to explore the relationship between calcium and ACh-stimulated release of glycine, samples were maintained in calcium-free medium containing 1 mM ethyleneglycol-bis-N,N,N',N'-tetraacetic acid as a chelating agent. The

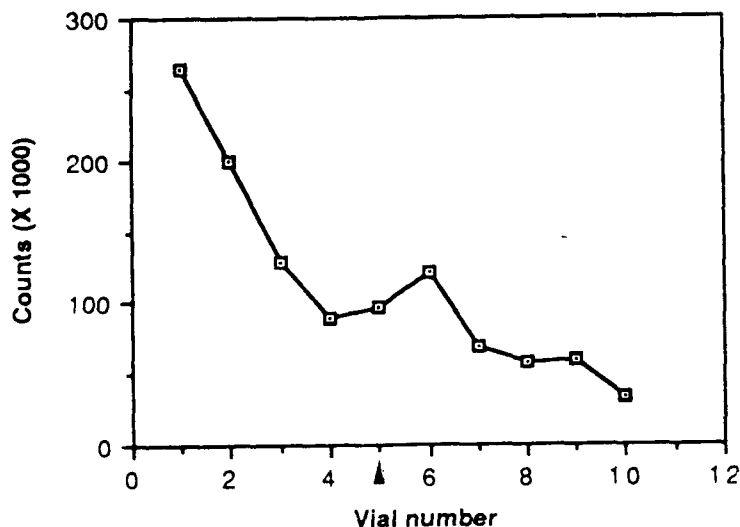


Fig. 12. ACh-stimulated release of (3H)glycine. The plot illustrates data from a single representative experiment. The ACh was added to the medium in vial 5 (arrowhead).

ACh added to samples containing the chelating agent was in the same calcium-free buffer.

Results. The basic experiment to determine whether ACh causes release of (3H)glycine was repeated 6 times with 3 clearly positive results, 2 apparent negatives, and 1 ambiguity. In spite of these rather diverse results, the overall pattern seen with ACh, and the absence of this response in the presence of blockers, seems to indicate that glycine release is triggered by ACh. This effect is illustrated in the curve shown in Fig. 12. Vials 1-4 illustrate the continuation of the wash-out of label from retinal tissue. An increased release of glycine was observed in vial 5 (which contained ACh) and vial 6. The wash-out pattern is restored in vials 7-10.

Samples preloaded with (3H)glycine but exposed to curare prior to application of ACh showed no increased release of glycine (Fig. 13). This result suggests that glycine release is mediated through the action of ACh on nicotinic receptors. Samples incubated in curare alone and never exposed to ACh showed some variability, with a large release of glycine in the later vials. Although not explored further, these findings suggest an independent toxic effect of curare on glycine-containing neurons. The increase in vial 8 of Fig. 13 may be explained in this manner. Samples treated with atropine showed an irregular release pattern in all vials, with escalating values in the early vials. There appeared to be no correlation with the addition of ACh.

The ACh-stimulated release of glycine was not observed in samples incubated in calcium-free medium containing the chelating agent EGTA. A plot of glycine release from such an experiment (Fig. 14) shows no increase in glycine in vial 5 concurrent with the application of ACh.

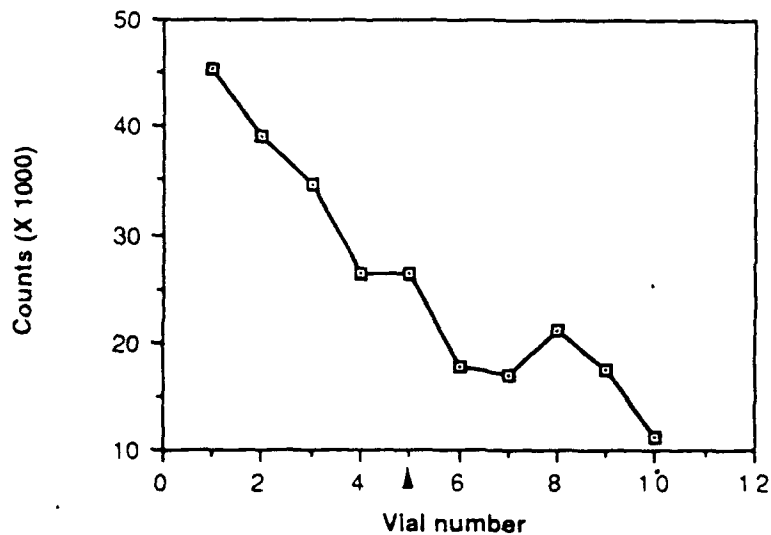


Fig. 13. ACh-stimulated release of (3H)glycine blocked by curare. Curare was present in the medium throughout the experiment. ACh was added in vial 5 (arrowhead). This plot is from a single representative experiment.

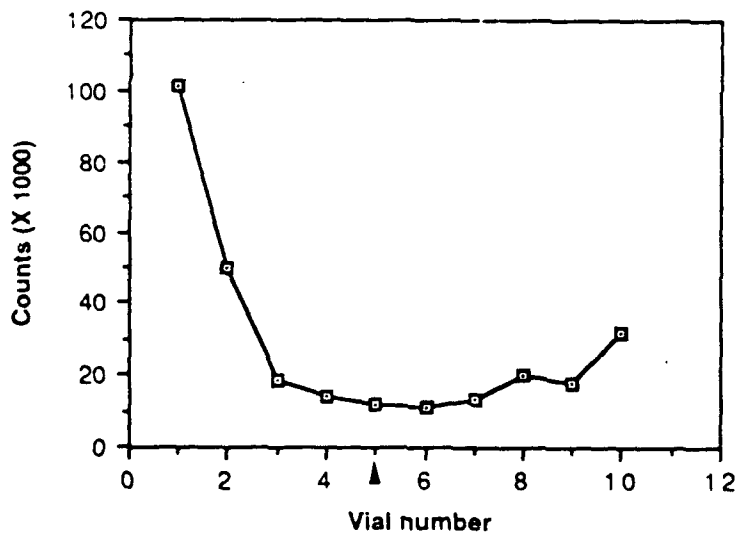


Fig. 14. Calcium dependence of (3H)glycine release. In a calcium-free medium, the addition of ACh in vial 5 (arrowhead) did not result in an increased release of (3H)glycine. This plot is from a single representative experiment.

Discussion. This study suggests that the action of ACh at nicotinic receptors stimulates the release of glycine from retinal neurons. From the present data, it is not possible to exclude the possibility of an involvement of muscarinic receptors also.

ACh-stimulated release of glycine was not observed when calcium was excluded from the medium. This appears to be a general phenomenon of glycine release, seen also in the monkey retina (11). The original goal in using calcium-free medium was to ascertain whether ACh-releasing cells were directly pre-synaptic to glycine-containing cells. Withdrawal of calcium would presumably have prevented the synaptic release of ACh and tested for the presence of ACh receptors directly on glycinergic neurons. However, since all glycine release appears to be calcium dependent, there is no basis in these experiments for distinguishing between direct and indirect cholinergic input to glycinergic cells. The findings do support concepts of neurochemical interactions and are of particular importance in indicating that alterations in the cholinergic system, induced by organophosphate poisoning, would cause widespread changes in other neurotransmitter systems.

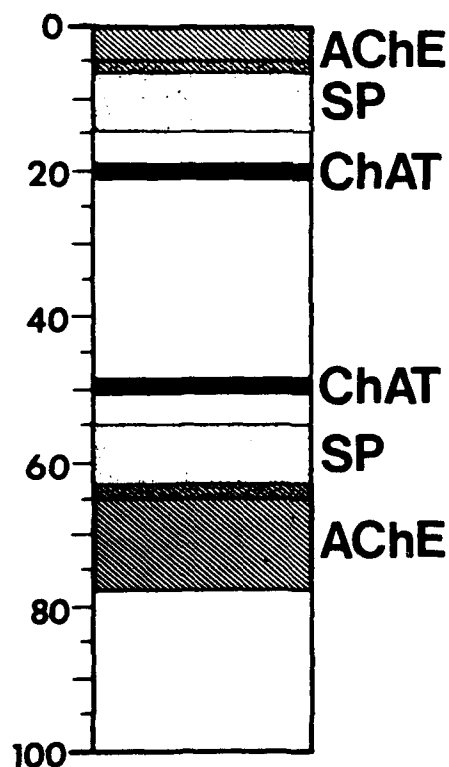


Fig. 15. Comparison of laminar distributions of ChAT, AChE, and SP in cat IPL. ChAT localizations at the 20 and 50% depth levels indicate the distribution of the dendrites of cholinergic neurons. AChE activity was present throughout the entire thickness of the IPL, but was found in the greatest concentration at 0-6% and 64-78%. SP immunoreactivity was seen at 5-15% and 55-65%.

2. Effects of anticholinesterase compounds on the neuropeptide SP.

Increasing evidence has accumulated to suggest that AChE has localizations and actions which extend beyond previously characterized cholinergic systems. One of the most interesting of the possible roles for AChE is the regulation of neuroactive peptides, particularly SP, as reported by Chubb et al. (7,8). Recent immunocytochemical studies of the cat retina have shown SP to be localized within amacrine and displaced amacrine cells (12). These cells ramify narrowly in strata 1 and 4 of the IPL. Both laminations border bands of intense AChE activity, but are not directly associated with the laminations of ChAT that mark the distribution of cholinergic processes (2,3). A comparison of the distributions of SP, AChE, and ChAT in the cat retina (Fig. 15) suggests a possible interaction of AChE with SP (along with its role in the classical esterase inactivation of ACh). If such an interaction occurs, one might expect a colocalization of AChE with SP. As reported previously, AChE activity is present in virtually every cell located within the cat GCL (3,4). Similar observations have been made in the rabbit retina. Since the majority of substance P-immunoreactive (SP-IR) cells in both species are located in the GCL, co-localization of SP and AChE appeared inevitable and has recently been verified in this laboratory.

In order to determine how changes in AChE activity might influence the level of SP, we injected animals with diisopropylfluorophosphate (DFP), a potent inhibitor of AChE, and then assayed the retinas for SP activity. Preliminary experiments with cat retinas proved unsuccessful due to the small amounts of the peptide in this species. However, rabbit retinas were found to contain levels of SP which are within the range for detection by standard radioimmunoassay (RIA) techniques, and so were used for these experiments.

Materials and Methods.

New Zealand white albino rabbits weighing 3-5 kg were anesthetized with pentobarbital prior to administration of DFP. One eye of each animal was injected intravitreally with 100 μ l DFP (1mg/ml in saline), while the companion uninjected eye served as a control. The rabbits were subjected to photostimulation by a white xenon strobe at 15 Hz, with normal room lighting as background for a 3-hour period to stimulate the cone pathway and minimize the endogenous release of ACh. At termination of the experiment, the animals were administered an overdose of pentobarbital and their eyes enucleated.

i) AChE staining of retinas

A small piece of each retina was fixed in 4% paraformaldehyde in 0.1M phosphate buffer for 2 hours followed by several rinses in phosphate buffered saline (PBS). These pieces were embedded in gelatin, frozen and

Table 1

Levels of SP-IR material in DFP-treated and untreated rabbit retinas

	Total amount of SP-IR/retina	Amount of SP-IR/ mg protein	Percent increase in DFP-treated retina
Experiment #1			
DFP-treated	87.5 pg	92 fg/mg	72%
Control	51.5 pg	54 fg/mg	
Experiment #2			
DFP-treated	67.5 pg	94 fg/mg	60%
Control	51.0 pg	57 fg/mg	
Experiment #3			
DFP-treated	142.5 pg	162 fg/mg	64%
Control	82.0 pg	99 fg/mg	
Experiment #4			
DFP-treated	108.5 pg	149 fg/mg	46%
Control	88.0 pg	102 fg/mg	
Experiment #5			
DFP-treated	84.4 pg	149 fg/mg	201%
Control	17.0 pg	74 fg/mg	
Experiment #6			
DFP-treated	28.0 pg	149 fg/mg	35%
Control	15.0 pg	110 fg/mg	

The amount of SP-IR material in both DFP-treated and control eyes was determined by RIA analysis. In each case, the amount of SP-IR material was greater in the DFP-treated retina, with an average increase of 80%.

sectioned into 20-um slices. AChE activity was detected cytochemically according to the method of VanOoteghem and Shipley (13).

ii) Crude extraction of SP-IR material

Retinas from both DFP-treated and untreated eyes were detached from the pigment epithelium, separated from the vitreous and placed in pre-weighed vials containing 1 ml of 0.1M HCl. The retinal samples were frozen over night at -20°C, thawed, homogenized and sonicated at 4°C. The crude preparation was centrifuged at 13,000 x g for 10 minutes with the supernatant saved for further processing. The pH was adjusted to 6.6 by the addition of 1% NaOH causing isoelectric precipitation of some of the larger proteins. The samples were then centrifuged at 12,000 x g for 2 minutes to pellet the precipitate and leave a clear supernatant preparation. The protein content of the final preparations was then determined with the use of a Pierce BCA protein assay kit utilizing a 30 min incubation at 37°C.

iii) Affinity purification of Retinal SP-IR material

To improve the purity of the samples, an affinity column was prepared by covalently linking a monoclonal antibody directed against SP (Pelfreeze) to cyanogen-bromide-activated sepharose 4B gel beads. The anti-SP-affinity column was equilibrated with 0.1M PBS and monitored at 280 nm. Each sample was diluted with 2 ml of 0.1 M PBS, then applied to the column head, then washed with PBS to re-establish baseline. The affinity coupled material was released from the gel bed by elution with 0.1M HCl. The fractions containing the released material were pooled and clarified by passing the contents through an activated Waters Sep-Pac C18 (Waters, Milford, MA). The hydrophobic material retained by the C18 cartridge was released with 1.5 ml of 100% acetonitrile. Each sample was diluted by the addition of 2 ml of water and then lyophilized.

iv) Radioimmunoassay (RIA) for SP-IR

Each lyophilized sample was rehydrated with 500 ul of BSA-peptone buffer (NCSTAR, Springwater, MN) and vortexed thoroughly. The samples were assayed with an RIA detection kit supplied by NCSTAR utilizing a standard protocol. In each experiment, samples were processed in pairs to compare the concentrations of SP-IR material in treated vs. untreated retinas.

Results. Before biochemical analysis, samples from both retinas of each animal were processed for cytochemical localization of endogenous AChE activity to assure that DFP inactivation affected only the target retina and not the control eye. In all cases, the AChE activity in the DFP-treated eyes was abolished while the untreated eye demonstrated strong AChE activity.

To determine if DFP had any effects on the levels of SP-IR material, each retina was sampled biochemically for SP-IR. The results (Table 1) show that all DFP treated retinas contained higher levels of SP-IR material than the untreated eyes from the same animal. To compare results

between DFP-treated vs. untreated retinas, the total amount of SP in each eye was divided by the protein content of the supernatant. These adjusted values were used to calculate the percent increase of SP in the DFP-treated eyes. DFP-treated retinas showed an average increase in SP-IR material of 80% increase as compared with untreated retinas.

Discussion. This study provides in vivo evidence for an interaction between DFP and SP. SP-IR activity in DFP-treated eyes was 35-200% greater than the levels found in control eyes from the same animals. These findings are consistent with a proteolytic role for AChE in the inactivation of SP. Small et al. (6,14) have recently shown that a subunit of AChE exhibits trypsin-like activity and acts as an endopeptidase on "model peptides". Furthermore, in earlier in vitro studies, Chubb et al. (8) and Lockridge (15) showed that purified AChE hydrolyzes SP. Inactivation of the enzyme by DFP abolished this hydrolysis. Similarly, in the present in vivo study, treatment of retinas with DFP caused an apparent decrease in proteolytic activity of AChE on SP. This led to an increase in the amount of SP-IR present after exposure to DFP.

Comparisons of the laminar distributions of SP and AChE in the retina also support the possibility of functional interactions of these two compounds. As previously reported, the major bands of AChE activity found in the IPL of the cat retina do not coincide with the banding patterns of ChAT-positive cells (1-4). However, SP-IR amacrine cell dendrites were found to ramify between the heavy AChE bands and the ChAT-positive bands in both sublamina a and b of the IPL (Fig. 15). This close association of SP-IR processes with AChE positive dendrites provides a morphological basis for the biochemical interaction. The case for interaction is further strengthened by preliminary studies in which we have colocalized AChE and SP-IR within the same retinal neurons.

While these findings appear to support a role for AChE in the hydrolysis of SP, other interpretations are also possible. DFP may have affected other proteases and enzymes in addition to inactivating AChE. The role of AChE is also uncertain. It has been suggested that AChE may serve as a posttranslational enzyme that hydrolyzes a larger tachykinin molecule to liberate SP. Millar and Chubb (7) reported that chicken retinas incubated in the presence of AChE showed an increased expression of both SP-IR and enkephalin immunoreactivity. However, if this were true in the rabbit retina, DFP would be expected to lower the levels of SP-IR in treated retinas below the amount found in control retinas. Another alternative is that endogenous levels of SP regulate a feedback mechanism for synthesis of SP through production of a precursor tachykinin molecule. In this model, AChE would cause an increase of an SP precursor that might be detectable by the immunological techniques used in these experiments. Further work will be required to determine which of these models most accurately describes the interaction between SP and AChE.

CONCLUSIONS:

Previous reports (1,3) have documented the identification of cholinergic neurons in the cat retina and the fact that AChE is present, not only in the cholinergic cells, but also in virtually all of the cells in the GCL. The cytochemical assay showed that all of the AChE activity is in the form of acetyl- and not butyrylcholinesterase. The AChE-positive cells include, but are not limited to, those neurons which are cholinceptive. Thus, AChE is distributed more widely than can be explained on the basis of its involvement in cholinergic transmission alone.

The present report has described the autoradiographic localization of both muscarinic and nicotinic receptors which, in support of earlier findings, indicated that cholinergic neurotransmission is confined primarily to the IPL. Autoradiographic localization of (3H)soman also showed a preferential distribution of binding sites within the IPL. The neurotoxic effects of soman were observed first in cells of the GCL and were seen to extend later into the outer layers of the retina. This distribution resembles more closely the distribution of AChE activity than that of ChAT. Thus, all neurons which contain AChE, and not only those cells which are cholinergic, appear to be at risk during exposure to soman.

The cholinergic system itself was shown to interact with other neurotransmitter systems in the retina. Application of ACh was demonstrated to cause an increased release of glycine.

In addition to its established role in the inactivation of ACh, AChE appears to have an enzymatic function in the hydrolysis of SP. This finding suggests that retinal levels of neuropeptides are at risk from exposure to anticholinesterase compounds. It is possible that deficits in neuropeptides may contribute to the longlasting effects of anticholinesterase compounds.

RECOMMENDATIONS:

The most important finding from this series of studies is the evidence that AChE, and the potential for its destruction by anticholinesterase compounds, extends beyond the neurons traditionally implicated in cholinergic neurotransmission. Further investigation of the non-cholinergic effects of AChE, particularly the effects on neuropeptide levels, is warranted. A priority should be an evaluation of the long-term effects of exposure to organophosphate compounds. After such a study is completed, it would be possible to test the effectiveness of commonly used antidotes in preventing or moderating these changes.

LITERATURE CITED

1. Pourcho, R.G., Annual Summary Report, Nov. 1984, Cholinergic neurotransmission in the mammalian retina, USAMRDC, Fort Detrick, Frederick, MD, DAMD17-83-C-3192.
2. Pourcho, R.G., and Osman, K. (1986) Cytochemical localization of cholinergic amacrine cells in cat retina, J. Comp. Neurol. 247, 497-504.
3. Pourcho, R.G., Annual Summary Report, Nov. 1985, Cholinergic neurotransmission in the mammalian retina, USAMRDC, Fort Detrick, Frederick, MD, DAMD17-83-C-3192.
4. Pourcho, R.G., and Osman, K. (1986) Acetylcholinesterase localization in cat retina: A comparison with choline acetyltransferase, Exp. Eye Res. 43, 585-594.
5. Pourcho, R.G., and Goebel, D.J. (1988) Colocalization of substance P and gamma-aminobutyric acid in amacrine cells of the cat retina, Brain Res. 447, 164-168.
6. Small, D.H., and Simpson, R.J. (1988) Acetylcholinesterase undergoes autolysis to generate trypsin-like activity, Neurosci. Lett. 89, 223-228.
7. Millar, T.J., and Chubb, I.W. (1984) Treatment of sections of chick retina with acetylcholinesterase increases enkephalin and substance P immunoreactivity, Neuroscience 12, 441-451.
8. Chubb, I.W., Hodgson, A.J., and White, G.H. (1980) Acetylcholinesterase hydrolyzes substance P, Neuroscience 5, 2065-2072.
9. Masland, R.H., and Livingstone, C.J. (1976) Effect of stimulation with light on synthesis and release of acetylcholine by an isolated mammalian retina, J. Neurophysiol. 39, 1210-1219.
10. Neal, M.J. (1983) Cholinergic mechanisms in the vertebrate retina, In Progress in Retinal Research, Vol 2, Eds., Osborne, N., and Chader, G., Pergamon Press, Oxford, pp. 191-212.
11. Hendrickson, A.E., Koontz, M.A., Pourcho, R.G., Sarthy, P.V., and Goebel, D.J., (1988) Localization of glycine-containing neurons in the macaca monkey retina, J. Comp. Neurol. 273, 473-487.
12. Pourcho, R.G., and Goebel, D.J., Substance P-like immunoreactive amacrine cells in the cat retina, J. Comp. Neurol. 275, 542-552.
13. VanOoteghem, S.A., and Shipley, M.T. (1984) Factors affecting the sensitivity and consistency of the

Koelle-Friedenwald histochemical method for localization of acetylcholinesterase, *Brain Res. Bull.* 12, 543-553.

14. Small, D.H., Ismael, Z., and Chubb, I.W. (1987) Acetylcholinesterase exhibits trypsin-like and metalloexopeptidase-like activity in cleaving a model peptide, *Neurosci.* 21, 991-995.

15. Lockridge, O. (1982) Substance P hydrolysis by human serum cholinesterase, *J. Neurochem.* 39, 106-110.

GLOSSARY

ACh	Acetylcholine
AChE	Acetylcholinesterase
Alpha-BTX	Alpha-bungarotoxin
ChAT	Choline acetyltransferase
CNS	Central nervous system
DFP	Diisopropylfluorophosphate
GCL	Ganglion cell layer
(3H)ACh	Tritiated acetylcholine
(3H)alpha-BTX	Tritiated alpha-bungarotoxin
(3H)choline	Tritiated choline
(3H)glycine	Tritiated glycine
(3H)PrBCM	Tritiated propylbenzyl choline mustard
HCl	Hydrochloric acid
INL	Inner nuclear layer
IPL	Inner plexiform layer
NFL	Nerve fiber layer
ONL	Outer nuclear layer
OPL	Outer plexiform layer
PBS	Phosphate buffered saline
PR	Photoreceptor outer and inner segments
RIA	Radioimmunoassay
SP	Substance P
SP-IR	Substance immunoreactive

